On the Response of the Ocean to a Moving Storm: Parameters and Scales

RICHARD J. GREATBATCH†

Department of Applied Mathematics and Theoretical Physics, University of Cambridge, Cambridge CB3 9EW England

(Manuscript received 8 June 1982, in final form 2 August 1983)

ABSTRACT

This paper has two purposes: One is to present a new and efficient multilevel numerical model for calculating the response of the ocean to a moving storm; the second is to show how, on a time scale of a few inertial periods following the arrival of the storm, the maximum horizontal and vertical velocities found in the wake can be calculated using a linear Ekman model and a knowledge of that part of the change in the depth of the wind mixed layer due to entrainment. This is demonstrated over a range of experiments with the multilevel numerical model. These integrate the full nonlinear equations of motion with realistic ocean stratification and involve substantial entrainment of water into the wind mixed layer.

It is also shown that on this time scale, the horizontal currents are confined near the surface but that the vertical velocity field extends throughout the depth of the ocean. It is shown in Appendix B that the wind forcing need only be "large" or "fast" for the forced response not to feel the effect of the ocean stratification and to extend through the depth of the ocean in this way.

The parameter which determines the horizontal structure of the response, in coordinates scaled with respect to the scale L of the storm, is $k = U/Lf$. Here U is the storm translation speed and f the Coriolis parameter. This parameter also determines the magnitude of the response, after suitable nondimensionalization.

Finally, it is shown how to apply these results to an interpretation of observations and other model results.

Introduction

The problem of the response of the ocean to a storm is, on the face of it, a complex one involving both storm scale dynamics and also substantial mixed layer effects. A number of models have been developed with which to study it. Most notable of these have been O'Brien and Reid (1967) and O'Brien (1967) who looked at stationary storms, O'Brien (1969) who looked at a slowly moving storm, Geisler (1970) who looked at the linear dynamics of the response to a moving storm but did not include mixed layer effects, Elsberry *et al.* (1976) who were primarily concerned with thermal effects and therefore placed emphasis on modeling the wind mixed layer, Chang and Anthes (1978) who combined mixed layer effects and dynamics in a one active layer model, Price (1981) who embedded a mixed layer model in a multilayer dynamical model and Martin (1982) who considered a one-dimensional model that included both dynamics and vertical mixing. This paper has two purposes: One is to present a new and efficient multilevel numerical model (in which a model for the wind-mixed layer has been embedded) for calculating the response to a moving storm; the second is to show how, on a time scale of a few inertial periods following the onset of the storm, the maximum horizontal and vertical velocities found in the wake of the storm can be calculated using a linear Ekman model and a knowledge of that part of the change in the mixed layer depth due to entrainment. This is demonstrated over a range of numerical experiments. These integrate the nonlinear equations of motion using realistic ocean stratification and involve substantial entrainment of water into the wind-mixed layer.

To achieve this second purpose, we consider the limit of large, fast storms introduced by Greatbatch (1984) and used there to elucidate those features of the response associated with the nonlinear terms in the equations of motion. The crucial approximation associated with this limit is that of dropping the horizontal pressure gradient terms from the equations of motion. Consideration of this limit leads to some additional results in this paper concerning the vertical structure of the response. In particular, it is found that the horizontal currents generated by the storm are initially confined near the surface, while the associated vertical velocity field extends throughout the depth of the ocean. In the large, fast storm limit this is just the inertial pumping[1] and varies linearly from the base of the wind-mixed layer to the ocean floor. In Appendix B, it is shown that it is sufficient that the wind forcing be either fast or large for the forced response to extend throughout the depth of the ocean in this way.

† Present affiliation: Geophysical Fluid Dynamics Program, Princeton University, Princeton, NJ 08540.

[1] By "inertial pumping" we mean the pumping associated with inertial currents in the mixed layer. This seems a more appropriate term to use than "Ekman pumping" since the latter usually refers to time scales long compared with $1/f$ and is given by assuming a steady state Ekman balance with the wind forcing.

The limit of large, fast storms is formally defined in Section 1 of this paper, following the setting up of the governing equations. The structure of the response in the large, fast storm limit is discussed in Section 2. The parameter which governs the response in this limit is $k = U/Lf$. This measures the ratio of the time scale L/U for the passage of the storm to the local inertial time scale $1/f$. Section 3 describes the multi-level numerical model which is used in Section 4 to generate results over many experiments. These are used to verify the conclusions of Section 2, showing that the numerically generated solutions are approximated quite well by the large, fast storm limit. Section 5 applies these ideas to give an interpretation of the model results of Price (1981) and also demonstrates that when considering observations or model results at a fixed point, it is important to consider the effects of horizontal advection. A summary and discussion is given in Section 6.

The paper also includes two appendices. In Appendix A, an alternative approach to the limit of large, fast storms is given which does not involve separating into vertical normal modes. Appendix B consists of a note on the depth of penetration of the ocean response to wind forcing. The aim here is twofold: 1) to find sufficient conditions under which the forced response is deep so that a description in terms of vertically propagating waves is inappropriate and 2) to demonstrate that it is the wave speeds associated with the baroclinic modes that measure the penetrability of the ocean and it can be misleading to consider only the upper highly stratified part of the ocean in isolation.

1. The equations

We consider a steady storm translating with speed U in the direction of x increasing. The forcing (X, Y) is then a function of the two independent variables $\xi = Ut - x$ and y, where t is time and y is the cross-track coordinate. It therefore makes sense to seek solutions that are functions only of ξ, y and z, where z is the vertical coordinate measured positively upwards, and this we shall do throughout this paper.[2] We shall ignore salinity effects so that instead of working with density ρ, we shall work with temperature T via the equation of state

$$\rho = \rho_0[1 - \alpha(T - T_0)],$$

where ρ_0 is the density at temperature T_0 and α the coefficient of thermal expansion whose value will be fixed at 2×10^{-4} °C^{-1}.

An important simplification in this paper will be to consider only the baroclinic response. In the context of the nonlinear equations to be considered, we shall define the barotropic response to be that associated with the vertically-averaged velocity field and the baroclinic to be that remaining when the barotropic is removed. Scale analysis can be used to show that it is reasonable to neglect the forcing of the baroclinic response due to the barotropic, provided the depth of the wind mixed layer h is small compared with the total depth H of the ocean and the scale of the storm is small compared with the barotropic Rossby radius of deformation. These conditions are generally satisfied in the open ocean. Indeed, throughout this paper, attention is restricted to the deep, open ocean in the sense that it is assumed that $h \ll H$ and that we are away from the influence of coastal boundaries and continental shelves. The equations for the baroclinic response in terms of the independent variables ξ, y and z are then

$$u_\xi(U - u) + \overline{uu_\xi} + vu_y + wu_z - fv = p_\xi + X + \overline{vu_y} + \overline{wu_z} + \left(\frac{du}{dt}\right)_{\text{mix}}, \quad (1.1a)$$

$$v_\xi(U - u) + \overline{uv_\xi} + vv_y + wv_z + fu = -p_y + Y + \overline{vv_y} + \overline{wv_z} + \left(\frac{dv}{dt}\right)_{\text{mix}}, \quad (1.1b)$$

$$0 = -p_z + g\alpha\theta, \quad (1.1c)$$

$$-u_\xi + v_y + w_z = 0, \quad (1.1d)$$

$$\theta_\xi(U - u) + v\theta_y + w(\theta + T)_z = \left(\frac{d}{dt}(\theta + T)\right)_{\text{mix}}, \quad (1.1e)$$

where the overbar denotes vertical average and $(d/dt)_{\text{mix}}$ denotes terms associated with turbulent mixing. Here $T(z)$ is the temperature of the ocean in its undisturbed state and θ the temperature perturbation from that state. Similarly, p is the perturbation pressure[3] divided by ρ_0. The velocity components (u, v, w) are in the x, y, z directions, respectively; g is the acceleration due to gravity and f the Coriolis parameter which is assumed to have a uniform value. The hydrostatic and Boussinesq approximations have been made, with ρ_0 being taken as a representative density.

Since the atmospheric surface pressure anomaly associated with the storm is only significant as a forcing of the barotropic mode [this is discussed by Geisler (1970)], it is neglected here. The forcing (X, Y) therefore consists only of wind forcing which will be modeled as a body force acting on a wind-mixed layer of depth h. We therefore have

[2] This simplification is crucial only to the numerical technique described in Section 3. It can be relaxed throughout the remainder of this paper.

[3] Throughout the rest of this paper, p will be called the perturbation pressure rather than the quantity $(\rho_0 p)$.

$$(X, Y) = \frac{1}{\rho_0 h}(\tau_x, \tau_y)F_v(z), \tag{1.2a}$$

where $\tau = (\tau_x, \tau_y)$ is the surface wind stress and

$$F_v(z) = \begin{cases} 1 - h/H, & -h \leqslant z \leqslant 0 \\ -h/H, & -H \leqslant z < -h. \end{cases} \tag{1.2b}$$

The projection of the wind forcing onto the barotropic mode has been removed so that (1.2) is the forcing appropriate to the baroclinic response.

Throughout this paper [and also Greatbatch (1984)], the wind mixed layer is modeled as a slab within which both horizontal currents and temperature are assumed to be uniform in the vertical. The depth h of this layer is given by the equation

$$Uh_\xi - (hu)_\xi + (hv)_y = \left(\frac{dh}{dt}\right)_{\text{mix}}, \tag{1.3}$$

where $(dh/dt)_{\text{mix}}$ is the rate of entrainment. It is assumed that all the mixing takes place in the form of entrainment of water into the wind mixed layer and that momentum is conserved in this process. The terms $(du/dt)_{\text{mix}}$, $(dv/dt)_{\text{mix}}$ in (1.1) are therefore zero everywhere except in the wind mixed layer where they are given by

$$\left(\frac{du}{dt}\right)_{\text{mix}} = -\frac{\Delta u}{h}\left(\frac{dh}{dt}\right)_{\text{mix}},$$

$$\left(\frac{dv}{dt}\right)_{\text{mix}} = -\frac{\Delta v}{h}\left(\frac{dh}{dt}\right)_{\text{mix}}. \tag{1.4}$$

$\Delta u = u_{\text{mix}} - u_{-h}$, $\Delta v = v_{\text{mix}} - v_{-h}$, is the difference in u, v, respectively, across the base of the layer, $(u_{\text{mix}}, v_{\text{mix}})$ being the horizontal velocity in the mixed layer itself.

a. Boundary and initial conditions

The equations (1.1) will be solved subject to the boundary conditions

$$w = 0 \quad \text{at} \quad z = 0, \tag{1.5a}$$

$$w = 0 \quad \text{at} \quad z = -H. \tag{1.5b}$$

Eq. (1.5a) is the rigid-lid approximation and is consistent with restriction to the baroclinic response.

To obtain an initial condition ahead of the storm, we note that in linear theory, the group velocity for internal waves is bounded above by the nonrotating wave speed c_1 associated with the first baroclinic mode. Typically c_1 has a value in the range between 1 and 3 m s^{-1}. When the storm translation speed U is greater than this, it follows that no disturbance will be felt ahead of the storm. This is the only situation we shall consider here. We therefore take as our initial condition

$$\left.\begin{aligned} u = v = w = p = \theta \equiv 0 \\ h = H_M \end{aligned}\right\} \tag{1.6}$$

ahead of the storm. In the context of the nonlinear equations, this will be correct provided U is greater than the wave speed c_1 associated with the undisturbed ocean ahead of the storm.

b. The limit of large, fast storms

Linearizing the equations (1.1) about the undisturbed state ahead of the storm and dropping the terms $(d/dt)_{\text{mix}}$ associated with turbulent mixing, we can use the boundary conditions (1.5) to separate the equations into vertical normal modes. This procedure is described in Gill and Clarke (1974) and in detail in Gill (1982). The equations for the horizontal structure of each mode are then just the linearized form of the forced shallow water equations studied by Greatbatch (1983). In particular, the scale analysis presented in Section 4 of that paper carries over directly to each mode. It follows immediately from the conclusions established there, that the horizontal pressure gradient terms p_ξ and p_y in (1.1) will be small compared with the Coriolis terms fv and fu, if

$$c_n^2/L^2f^2 \ll 1, \tag{1.7a}$$

$$c_n^2/U^2 \ll 1, \tag{1.7b}$$

where c_n is the nonrotating wave speed associated with the nth mode, L is a length scale characteristic of the half-width of the response across the storm track and the conditions (1.7) are to be satisfied for each baroclinic mode (i.e., for $n \geqslant 1$). We note that since the wave speeds c_n are such that $c_1 > c_2 > \cdots > c_{n-1} > c_n > c_{n+1} > \cdots$, the conditions (1.7) need only be satisfied for the first baroclinic mode to be satisfied for all baroclinic modes.

The conditions (1.7a) and (1.7b) correspond to large and fast storms, respectively. In the limit of large and fast storms, the terms p_ξ and p_y will be dropped from (1.1), this being taken as a definition. It is important to appreciate that the dispersion of energy either out from the storm track or down from the mixed layer into the thermocline is absent in this limit, these processes being crucially dependent on the neglected terms p_ξ and p_y. It follows that consideration of this limit cannot provide useful information on time scales characteristic of the dispersion process; i.e., typically about five inertial periods or longer (see Price, 1983).

2. The response in the limit of large, fast storms

Throughout this section, the horizontal pressure gradient terms p_ξ and p_y will be dropped from (1.1a) and (1.1b) in accordance with the definition of the limit of large, fast storms given at the end of the previous section. It should be noted that the numerical model, to be described in Section 3, which is used to

generate the results discussed in Section 4 integrates the full system (1.1), including these terms.

We begin by considering the linearized equations about the undisturbed state ahead of the storm. These are

$$Uu_\xi - fv = X, \tag{2.1a}$$

$$Uv_\xi + fu = Y, \tag{2.1b}$$

$$0 = -p_z + g\alpha\theta, \tag{2.1c}$$

$$-u_\xi + v_y + w_z = 0, \tag{2.1d}$$

$$U\theta_\xi + (N^2/g\alpha)w = 0. \tag{2.1e}$$

The mixing terms $(d/dt)_{\text{mix}}$ have been temporarily dropped—their effect will be included later. This means, in particular, that the mixed layer depth h which appears in the expression for the forcing (1.2) is, for the time being, fixed at the undisturbed depth H_M; $N^2 = g\alpha T_z$ is the square of the buoyancy frequency. If L is the horizontal scale of the storm (which is assumed to be radially symmetric), it follows immediately that the solution to (2.1) can be written in the form

$$(u, v) = (\tau_{\max} L/\rho_0 H_M U) F_v(z)(u_H, v_H), \tag{2.2a}$$

$$w = (\tau_{\max}/\rho_0 U) G_v(z) w_H, \tag{2.2b}$$

$$\theta = (\tau_{\max}/\rho_0 Uf)\frac{N_0^2}{g\alpha}\Theta_v(z)\theta_H, \tag{2.2c}$$

$$p = (\tau_{\max}/\rho_0 Uf) N_0^2 H_T P_v(z)\theta_H, \tag{2.2d}$$

where

$$F_v(z) = \begin{cases} 1 - H_M/H, & -H_M \leqslant z \leqslant 0 \\ -H_M/H, & -H \leqslant z \leqslant -H_M, \end{cases} \tag{2.3a}$$

$$G_v(z) = \begin{cases} (1 - H_M/H)z/H_M, & -H_M \leqslant z \leqslant 0 \\ -(z + H)/H, & -H \leqslant z \leqslant -H_M, \end{cases} \tag{2.3b}$$

$$\Theta_v(z) = \frac{N^2(z)}{N_0^2} G_v(z), \tag{2.3c}$$

$$P_v(z) = \frac{1}{H_T}\int_{z_0}^{z} \Theta_v(z)dz, \tag{2.3d}$$

where H_T is the vertical scale of the thermocline. Use has been made of the boundary and initial conditions (1.5) and (1.6) and z_0 is chosen so that $P_v(z)$ has zero vertical average, a necessary requirement of restricting to the baroclinic modes only. The point of writing the solution in this form is that the nondimensional variables u_H, v_H, w_H and θ_H depend only on the horizontal coordinates y and ξ and the single nondimensional parameter

$$k = \frac{U}{Lf}. \tag{2.4}$$

In particular, the horizontal structure of the response, in coordinates scaled with respect to the scale L of the storm, is seen to depend only on k. Here k^{-1} measures the time scale for the passage of the storm L/U in units of the local inertial time scale $1/f$ and can be conveniently labeled the "passing time" of the storm, large k corresponding to short passing time.[4] Note that although k can take a range of values, it can be near unity, in which case we have an inertial resonance. For example, letting $U = 5$ m s^{-1}, $L = 75$ km and $f = 7.5 \times 10^{-5}$ s^{-1} gives $k = 0.9$. Since it is clear from (2.1a) and (2.1b) that L is also the cross-track scale of the response, it follows that k also measures the ratio of the along-track to the cross-track scales of the oscillations in the wake behind the storm.

The vertical structure of the response in (2.2) is given by the functions $F_v(z)$, $G_v(z)$, $\Theta_v(z)$ and $P_v(z)$. Hence for the deep ocean, $H_M \ll H$, the horizontal currents, with vertical structure given by F_v, are seen to be confined to the surface Ekman layer of depth H_M. Associated with these currents is the corresponding vertical velocity field given by (2.2b). This is just the inertial pumping. It is seen to extend throughout the depth of the ocean varying linearly from the base of the Ekman layer to the ocean floor. This large vertical scale for the w field was a feature of the model results of Price (1983, 1984) and also seems to be a feature of the observational studies described in Price (1981). In particular, the upwelling was often found to be in phase with depth deep into the main thermocline. A particularly fine example is provided by the study of the response to Typhoon Phyllis of 1975 described in Schramm (1979). In this case, the upwelling appears to be almost in phase throughout the thermocline with no apparent decay with depth over the 300 m covered by the observations.

We shall now allow the mixed layer depth h to vary by including the effects of vertical advection and entrainment but neglecting the horizontal advection. We shall see in Section 4 that this simplification is a reasonable one in that the conclusions of the following analysis are found to apply in the case of numerical experiments which include horizontal advection. It is clear that provided $h \ll H$, i.e., we are in the deep ocean, as before, we can consider the mixed layer in isolation from the ocean below, which can be taken

[4] In Price (1984), k is the nondimensional storm speed S. Note that whereas Price refers to a fast storm as being one for which $k \gg 1$, in this paper a fast storm is one for which $U^2 \gg c^2$ as in (1.7b). Note that a storm can be large and fast in the sense that $L^2f^2/c^2 \gg 1$ and $U^2/c^2 \gg 1$ [as in (1.7)] but $k = (U/c)/(Lf/c)$ can be less than or greater than 1.

to have no horizontal motion. The equations that describe the wind mixed layer are then

$$Uu_\xi - fv = \frac{\tau_x}{\rho_0 h} - \frac{u}{h}\left(\frac{dh}{dt}\right)_{\text{mix}}, \tag{2.5a}$$

$$Uv_\xi + fu = \frac{\tau_y}{\rho_0 h} - \frac{v}{h}\left(\frac{dh}{dt}\right)_{\text{mix}}, \tag{2.5b}$$

$$Uh_\xi + h(-u_\xi + v_y) = \left(\frac{dh}{dt}\right)_{\text{mix}}. \tag{2.5c}$$

It is convenient to separate h in two parts: h_E for which changes are associated with entrainment and h_D, associated with vertical advection, i.e., upwelling. We, therefore, define h_E by

$$Uh_{E\xi} = \left(\frac{dh}{dt}\right)_{\text{mix}}; \quad h_E|_{\text{ahead of storm}} = H_M \tag{2.6a}$$

and h_D by

$$Uh_{D\xi} = h(-u_\xi + v_y); \quad h_D|_{\text{ahead of storm}} = 0. \tag{2.6b}$$

Note that $h = h_E - h_D$. Combining (2.5a), (2.5b) and (2.6a) gives

$$U(h_E u)_\xi - f(h_E v) = \frac{1}{\left(1 - \frac{h_D}{h_E}\right)}\left\{\frac{\tau_x}{\rho_0} - u\left(\frac{dh}{dt}\right)_{\text{mix}}\right\} + u\left(\frac{dh}{dt}\right)_{\text{mix}}, \tag{2.7a}$$

$$U(h_E v)_\xi + f(h_E u) = \frac{1}{\left(1 - \frac{h_D}{h_E}\right)}\left\{\frac{\tau_y}{\rho_0} - v\left(\frac{dh}{dt}\right)_{\text{mix}}\right\} + v\left(\frac{dh}{dt}\right)_{\text{mix}}, \tag{2.7b}$$

which in the limit $h_D/h_E \to 0$ reduces to

$$U(h_E u)_\xi - f(h_E v) = \frac{\tau_x}{\rho_0}, \tag{2.8a}$$

$$U(h_E v)_\xi + f(h_E u) = \frac{\tau_y}{\rho_0}. \tag{2.8b}$$

The equations (2.8) are effectively just (2.1a) and (2.1b) but with the constant Ekman layer depth H_M replaced by the variable depth h_E from which it follows that the solutions to (2.8) can be written in the form

$$(u, v) = \left(\frac{\tau_{\max} L}{\rho_0 h_E U}\right)(u_H, v_H), \tag{2.9}$$

[cf. (2.2a)].

Equation (2.9) is fundamental to achieving the second purpose of this paper—that of showing how to calculate the maximum horizontal and vertical velocities found in the wake of the storm using a linear Ekman model and a knowledge of that part of the change in the mixed layer depth due to entrainment. This latter is represented in (2.9) by h_E, the former by the function (u_H, v_H). Indeed, it should be noted that the function (u_H, v_H) in (2.9) is the same as (u_H, v_H) in (2.2a) and satisfies the linear Ekman equations (2.1a) and (2.1b). We shall use (u_H, v_H) and w_H to define two further functions that are easily calculated using (2.1a) and (2.1b) given the surface wind stress field (τ_x, τ_y). These functions are $V_M(k)$ and $W_M(k)$ given by

$$V_M(k) = \underset{\text{of storm}}{\text{max wake}}\{(u_H^2 + v_H^2)^{1/2}\}, \tag{2.10a}$$

$$W_M(k) = \underset{\text{of storm}}{\text{max wake}}\{|w_H|\}. \tag{2.10b}$$

Here the maxima are taken over the wake, behind the storm and it is clear that both V_M and W_M depend only on k. We shall find in Section 4 (see Table 2) that, to a very good approximation the maximum horizontal current $V_{\max}$ found in the wake of the storm in each of the numerical experiments considered is given by

$$V_{\max} = \left[\frac{\tau_{\max} L}{\rho_0 (H_M + \Delta h) U}\right] V_M(k), \tag{2.11}$$

where here Δh is the maximum entrainment found following a material column of fluid in the wind-mixed layer. In fact, $(H_M + \Delta h)$ is the maximum value of h_E found in the wake of the storm where now h_E is defined by

$$\frac{Dh_E}{Dt} = \left(\frac{dh}{dt}\right)_{\text{mix}}; \quad h_E|_{\text{ahead of storm}} = H_M. \tag{2.12}$$

Here (D/Dt) is the total derivative following a fluid particle and (2.12) is the extension of (2.6a) when horizontal advection is included. It is important to realize that (2.11) is found to hold in experiments that include horizontal advection. It is clear that (2.11) is a natural extension from (2.9).

In extending (2.9) to calculate the vertical velocity field w in the wake, account must be taken of the cross-track variation of h_E. In fact, substituting (2.9) into the continuity equation (2.1d) and integrating down from $z = 0$, where $w = 0$, we obtain

$$w = \left(\frac{\tau_{\max}}{\rho_0 U}\right)\left[\frac{h}{h_E} w_H + L\left(\frac{1}{h_E}\right)_y v_H\right]\frac{z}{h}, \quad -h \leqslant z \leqslant 0. \tag{2.13}$$

It turns out that a good approximation for the maximum at depth $-z$ in the wake, $W_{\max}$, can be obtained by neglecting $[L(1/h_E)_y v_H]$ and is in fact given by

$$W_{\max} = \left(\frac{\tau_{\max}}{\rho_0 U}\right)\left\{\frac{-z}{(H_M + \Delta h)}\right\} W_M(k),$$

$$-h \leqslant z \leqslant 0, \qquad (2.14)$$

where $(H_M + \Delta h)$ is again the maximum value of h_E defined by (2.12) found in the wake. As before, this is verified in Section 4 over a range of experiments that include horizontal advection (see Table 3).

It is apparent from the foregoing discussion that horizontal advection does not appear to have any significant influence on the magnitude of the response. However, it can affect the horizontal structure as described in Greatbatch (1983), though not in a way that is more than a distortion by means of advection of the linear picture. A case in which it is important to consider horizontal advection is when interpreting observations or model results at a fixed point as demonstrated at the end of Section 5. Two parameters A_T and P_T were introduced in Greatbatch (1983) which measure the importance of the along-track and cross-track advection terms, respectively, in the equations of motion. These are given by

$$A_T = \frac{V}{U}; \quad P_T = \frac{V}{Lf}, \qquad (2.15)$$

where V is a scale for the horizontal velocity (these parameters arise when the cross-track coordinate is scaled by L and the along-track coordinate by U/f). The importance of horizontal advection in the wake of the storm can now be assessed by taking V to be the maximum horizontal current found in the wake of the storm, i.e., $V_{\max}$ given by (2.11). We then have

$$A_T = \left\{\frac{\tau_{\max} L}{\rho_0 (H_M + \Delta h) U^2}\right\} V_M(k), \qquad (2.16a)$$

$$P_T = \left\{\frac{\tau_{\max}}{\rho_0 (H_M + \Delta h) U f}\right\} V_M(k). \qquad (2.16b)$$

It is clear from (2.16) that, all other factors remaining the same, the importance of horizontal advection decreases as the storm translation speed U increases (note that $k = U/Lf$ can be allowed to vary, keeping L and f fixed, since as we shall see, $V_M(k)$ has only a weak dependence on k for $k \geqslant 1$ and is in fact bounded above throughout this range).

The remainder of Section 2 is concerned with the variation of the functions V_M and W_M with k and with giving the method that is used here and in Greatbatch (1984) for choosing the scale L of the storm. Readers who are not concerned with these details can proceed to Section 3.

a. *The variation with* k

We return to the linearized equations (2.1) and consider the dependence of V_M and W_M defined by (2.10) on k. Only the wake behind the storm will be considered. The wind forcing (X, Y) is here modeled using trigonometric functions, essentially corresponding to a single Fourier mode. We therefore put

$$(X, Y) = \frac{\tau_{\max} F_v(z)}{\rho_0 H_M} \begin{cases} \left[-\sin\left(\frac{\pi y}{2L}\right)\cos\left(\frac{\pi \xi}{4L}\right), -\cos\left(\frac{\pi y}{4L}\right)\sin\left(\frac{\pi \xi}{2L}\right)\right], & (|y|, |\xi| \leqslant 2L) \\ 0, & \text{otherwise,} \end{cases} \qquad (2.17)$$

where here L has been chosen to be the half-width of the region in which positive vorticity is imparted by the storm which is also the half-width of the region of net upwelling due to the storm. The forcing (2.17) will be used later as a standard by which L can be chosen for an arbitrary storm.

It is an easy matter to solve (2.1a) and (2.1b) with (X, Y) given by (2.17) and with the initial condition $u = v = 0$ for $\xi \leqslant -2L$. The function (u_H, v_H) can be written in the wake of the storm as

$$(u_H, v_H) = \left\{A(k)\sin\left(\frac{\pi}{2} ky^*\right) + B(k)\cos\left(\frac{\pi}{4} ky^*\right)\right\} \times (\cos\xi^*, -\sin\xi^*),$$

where $\xi^* = f\xi/U$, $y^* = fy/U$ and $k = U/Lf$. $V_M(k)$, given by (2.10a), is now found by maximizing

$$\left[A(k)\sin\left(\frac{\pi}{2} ky^*\right) + B(k)\cos\left(\frac{\pi}{4} ky^*\right)\right]$$

as a function of y^* and this maximum is plotted as a function of k in Fig. 1a (solid line). Having obtained (u_H, v_H) we can now find w_H using (2.1d). The maximum of $|w_H|$ in the wake of the storm, $W_M(k)$, (here also restricted to being along the storm track) is shown in Fig. 1b (solid line).

The initial peak in both curves as k increases corresponds to the inertial resonance referred to earlier. For values of k greater than the resonance value, the dependence on k shown in Fig. 1 is comparatively weak. It is of interest to consider what determines the limiting values as $k \to \infty$. In the case of $V_M(k)$, this obviously depends on the choice of L. For $W_M(k)$ it is independent of L [cf. (2.2a) and (2.2b)].

b. *The limit* k $\to \infty$*: A method for choosing* L

The functions (u_H, v_H) are now given by

$$Uu_{H\xi} - fv_H = 0; \quad Uv_{H\xi} + fu_H = 0$$

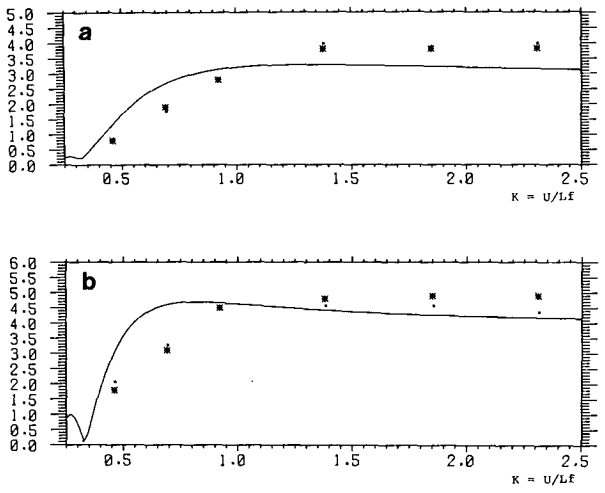

FIG. 1. (a) The maximum surface current found in the wake of the storm, nondimensionalized with respect to $(\tau_{max}L/\rho_0 UH_M)F_v(z)$ and plotted as a function of $k = U/Lf$. The solid line was obtained analytically using the wind forcing (2.17). The points marked by an asterisk and a dot are the results of linear and nonlinear numerical experiments without mixing (experiments 7–12, inclusive, in Table 1), respectively; (b) as in (a), except for the maximum vertical velocity found in the wake of the storm, nondimensionalized with respect to $(\tau_{max}/\rho_0 U)G_v(z)$.

subject to

$$\left.\begin{aligned} u_H|_{\xi=0} &= \frac{1}{L}\int_0^{\xi_0} X'd\xi \equiv u_0, \quad \text{say} \\ v_H|_{\xi=0} &= \frac{1}{L}\int_0^{\xi_0} Y'd\xi \equiv v_0, \quad \text{say} \end{aligned}\right\}, \tag{2.18}$$

where $0 \leqslant \xi \leqslant \xi_0$ encloses the storm and (X', Y') is the forcing nondimensionalized with respect to $(\tau_{max}/\rho_0 H_M)Fv(z)$. It follows immediately that

$$\left.\begin{aligned} u_H &= u_0 \cos\left(\frac{f\xi}{U}\right) + v_0 \sin\left(\frac{f\xi}{U}\right) \\ v_H &= -u_0 \sin\left(\frac{f\xi}{U}\right) + v_0 \cos\left(\frac{f\xi}{U}\right) \end{aligned}\right\} \tag{2.19}$$

and hence that

$$\lim_{k\to\infty} V_M(k) = \max_y [(u_0^2 + v_0^2)^{1/2}], \tag{2.20}$$

where the maximum in (2.20) is taken over the range of y.

When (X, Y) is given by (2.17), $v_0 = 0$ and so

$$\lim_{k\to\infty} V_M(k) = \max_y |u_0| = 8/\pi \approx 2.55$$

It is important to realize that its precise value depends crucially on how L is chosen. The dimensional quantity

$$L\max_y[(u_0^2 + v_0^2)^{1/2}]$$

is however, dependent only on the storm [cf. (2.18)], and it is always possible to choose L so that $\max_y[(u_0^2 + v_0^2)^{1/2}]$, and hence $\lim_{k\to\infty} V_M(k)$, is equal to $8/\pi$. *This is the method used to choose* L *in this paper.*

In the limit $k \to \infty$, i.e., $U/f \gg L$, only derivatives in the cross-track coordinate y will be important in determining the divergence. It follows that

$$w_H = -v_{Hy'}$$

where $y' = y/L$ and hence

$$w_H = -v_{0y'} \cos\left(\frac{f\xi}{U}\right) + u_{0y'} \sin\left(\frac{f\xi}{U}\right).$$

It follows that

$$\lim_{k\to\infty} W_M(k) = \max_y[(v_{0y'}^2 + u_{0y'}^2)]. \tag{2.21}$$

When (X, Y) is given by (2.17) [and the maximum in (2.21) is further restricted to the storm track $y = 0$ so as to afford comparison with the solid curve in Fig. 1b], this value is 4. In this case, the value is independent of how L is chosen. It is, however, dependent on the horizontal structure of the storm—the value 4 is not unique.

The fact that $W_M(k)$ is independent of L, except insofar as it depends on $k = U/Lf$, has an interesting consequence that will be referred to in Greatbatch (1984). It might be thought that increasing the horizontal scale L of the storm, keeping all other factors constant and so decreasing the positive wind stress curl in the core of the storm would decrease the vertical velocity. However, the weak dependence of W_M on k in the range $k \gtrsim 1$ means that within this range this is not true [using (2.2b) and (2.10b) the magnitude of w is given by $(\tau_{max}/\rho_0 U)W_M(k)$]. Increasing L, keeping τ_{max}, U and f fixed decreases k only. This apparent paradox arises because the storm is moving—it is not true for a stationary storm. In fact, we can see from (2.21) [using the definition of u_0 and v_0, (2.18)] that it is the integrated wind stress curl (in the case of u_0) and wind stress divergence (in the case of v_0) that are important. It is usual for the wind stress curl to dominate, and so we can see that the value of $W_M(k)$ can be comparable both for a storm with a tight core of large positive wind stress curl and for a storm in which the positive wind stress curl is less but distributed over a wider area.

3. An efficient numerical model

In this section a novel and efficient numerical model is described for integrating the equations (1.1). Both the novelty and the efficiency come from seeking solutions that are in a steady state translating in equilibrium with the storm; i.e., working with the independent variables ξ, y and z. (The method has already

been used by Greatbatch (1983) in a case where there is no z dependence.) The basic approach is then to solve (1.1) as an initial value problem in the time variable ξ with initial condition (1.6) applied at the leading edge of the storm. The method can be thought of as either integrating to find the time development of the solution on a vertical cross section perpendicular to the storm track or integrating backwards along the storm track to find the spatial distribution of the solution at a given time. It is clear that considerable savings in computer resources are achieved by combining the along-track coordinate and the time dependence into the single coordinate ξ.

The model ocean consists of a stack of fixed levels of variable thickness. The temperature T and vertical velocity w are stored at the edge of each level and the variables u, v, p at the centers. The variables are stored horizontally according to the Arakawa C-grid (Arakawa and Lamb, 1977) with u, p, w and T at the same horizontal position and v at intermediate points. The leap-frog scheme is used in time (ξ) with second-order centered differencing in space (y, z).

In discussing how we solve the resulting finite difference equations we will drop both the mixing terms $(d/dt)_{\text{mix}}$ and the terms uu_ξ etc. The method for dealing with the former will be discussed in detail in Greatbatch (1984)[5] and the latter terms are readily incorporated by means of inverting a simple matrix.

A basic problem with solving the finite difference form of (1.1), when the leap-frog scheme is used in time ξ, is that the vertical velocity w needed to update the temperature θ via (1.1e) is dependent on the new value of the velocity component u because of the continuity equation (1.1d). This problem can be overcome if the vertical temperature gradient $(\theta + T)_z$ is always nonzero everywhere, in which case the finite difference equations can be solved exactly. To see this, we note that w can be expressed in terms of the perturbation pressure p using (1.1e) and (1.1c). When this expression for w is substituted into (1.1d), we obtain

$$u_\xi + \left[\frac{\frac{p_{z\xi}}{g\alpha}(U-u) + v\theta_y}{(\theta+T)_z}\right]_z = v_y. \qquad (3.1)$$

We can then eliminate u_ξ between (1.1a) and (3.1) to give an ordinary differential equation in z for p. The corresponding finite difference form of this equation is then solved at each time step for the new value of p subject to p having zero vertical average (corresponding to restricting only to the baroclinic modes). The new value of u is then obtained from either (1.1a) or (3.1) enabling w to be diagnosed from the finite difference forms of (1.1c) and (1.1e), respectively.

The above method is dependent on $(\theta + T)_z$ being always nonzero everywhere. However, we shall want to integrate (1.1) in cases when we have a surface mixed layer in which it will be assumed that the vertical gradient of temperature, $(\theta + T)_z$, is indeed zero. In this case, an iterative method is used to find w starting with the most recently calculated values which are used to integrate (1.1e) to give a first guess for θ and hence p. This then enables a new u field to be found from (1.1a) which can be substituted into (1.1d) to give a second guess for w. This process is then repeated until the solution converges. In practice, only three iterations are usually necessary.

Both methods can be compared in cases where $(\theta + T)_z$ is always nonzero everywhere. In test cases, the results have been found to be indistinguishable.

The accuracy and properties of the finite difference scheme are discussed in Greatbatch (1980). In particular, the solutions found by Geisler (1970) have been reproduced.

4. Numerical experiments

In this section, we describe experiments using the numerical technique presented in the previous section to integrate the equations (1.1).

The vertical temperature profile ahead of the storm is given by

$$T\,[^\circ\text{C}] = \begin{cases} 28.61, & (-35\text{ m} \leqslant z \leqslant 0) \\ \left\{5.02 - \ln\left[\dfrac{(-z+10)}{9.75}\right]\right\}\Big/0.122, & \\ \qquad -550\text{ m} \leqslant z \leqslant -35\text{ m} & \\ 4 + 4(z+2000)/1450, & \\ \qquad -2000\text{ m} \leqslant z \leqslant -550\text{ m}, & \end{cases} \qquad (4.1)$$

the total depth of the ocean being fixed at 2000 m. The structure above 550 m is a least squares fit to data from the EB-10 buoy prior to the passage of Hurricane Eloise in 1975 [Johnson and Withee (1978)] using a method described by Friese (1977). This structure is shown in Fig. 2, together with the grid levels used in the numerical model. The initial mixed layer depth is 35 m.

The surface wind stress τ is given by

$$\tau \equiv (\tau_r, \tau_\theta) = (-\tau_{r\max}, \tau_{\theta\max}) \begin{cases} \dfrac{r}{r_M}, & 0 \leqslant r \leqslant r_M \\ \dfrac{r_0 - r}{r_0 - r_M}, & r_M \leqslant r \leqslant r_0 \\ 0, & r_0 \leqslant r, \end{cases} \qquad (4.2)$$

[5] The fields of u, v and T are first updated with $(d/dt)_{\text{mix}} \equiv 0$. These updated fields are then "mixed" before being returned to the model. In the case of u and v, this involves redistributing the momentum of the updated field over the new mixed layer depth h [this is equivalent to the form of $(du/dt)_{\text{mix}}$ and $(dv/dt)_{\text{mix}}$ given in (1.4)].

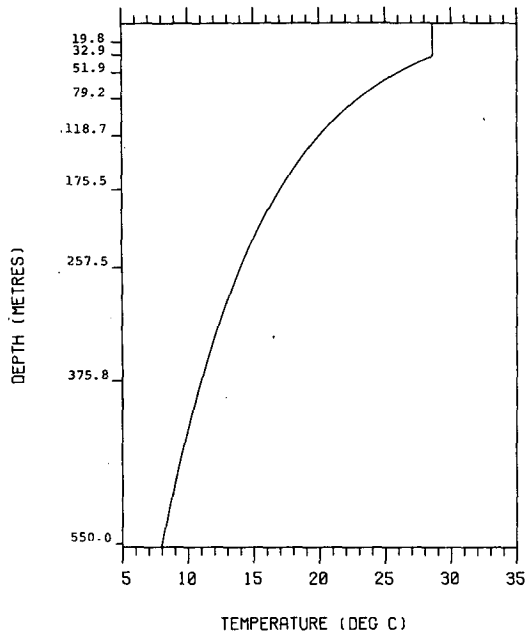

FIG. 2. The temperature structure for the upper 550 m of the undisturbed ocean ahead of the storm used in the model experiments. The vertical resolution is shown down the left-hand side.

where τ_r and τ_θ are the radial and tangential components of the stress with respect to the storm center and r is the radial distance from the center. We put $\tau_{r_{\max}} = 1\ \mathrm{Nm}^{-2}$, $\tau_{\theta_{\max}} = 3\ \mathrm{Nm}^{-2}$ and $r_0 = 10r_M$. The choice of r_M, the radius of maximum winds, sets the horizontal scale of the forcing.

Throughout all the experiments, the cross-track grid spacing Δy is fixed at $r_0/14.5$. This is 20.7 km in all experiments except experiments 3, 7 and 8 (see Table 1) for which it is 41.4 km. The along-track grid spacing $\Delta\xi$ is fixed at $\frac{3}{4}$ of this. In test experiments, the solutions were not found to be significantly changed when the resolution is doubled.

Twelve levels are used in the vertical with the base of each level being at depths of 19.8, 32.9, 51.9, 79.2, 118.7, 175.5, 257.5, 375.8, 550, 1000, 1500 and 2000 m. The depths above 550 m were obtained from the logarithmic profile in (4.1) by taking an interval of 3°C across each level.

Each integration was run for 60 time steps, corresponding to an along-track distance of 931 km (1862 km in experiments 3, 7 and 8). Free-slip boundary conditions are applied at the edges of the cross-track grid (i.e., zero normal velocity and zero flux). In test cases, no significant reflection was found on the time scale considered here.

a. Model experiments

Twelve experiments are considered, each in linear and nonlinear versions without mixing and a nonlinear version with mixing that integrates the full equations (1.1). In all the experiments, the wind forcing is modeled as a body force acting on a surface Ekman layer. In the linear and nonlinear experiments without mixing, this is kept fixed at depths of 35 and 50 m, respectively. In the experiments that include mixing, this depth is just the mixed layer depth h as in (1.2a), with h being given by (1.3) with initial value 35 m. The rate of entrainment $(dh/dt)_{\mathrm{mix}}$ is parameterized following Gill and Turner (1976) using the implementation for a model with fixed grid levels in the vertical (as here) described in Wells (1979). A detailed discussion of this is given in Greatbatch (1984).

The twelve experiments are summarized in Table 1. They are divided into three groups: experiments 1, 2 and 3 for which $k = U/fL$ has value 0.92; experiments 4, 5 and 6 for which $k = 1.85$ and experiments 7, 8, 9, 10, 11 and 12 which cover a range of values of k. The scale L used to define k has been chosen so that $\lim_{k\to\infty} V_M(k)$ is the same for both the stress field (4.2) used in the numerical experiments and for the stress field (2.17) as described in the previous section. This gives

$$L = 2.4r_M. \tag{4.3}$$

It should be realized that the factor 2.4 is dependent on the detailed structure of the storm and is special to the wind stress field (4.2). The values of k appropriate to each experiment, calculated with this scale, are given in Table 1. Note that experiments 9 and 11 are the same as experiments 1 and 4, respectively.

b. Model results

1) VERIFICATION OF (2.11) AND (2.14)

The maximum horizontal current and vertical velocity found in the wake of the storm at depths of 9.9 and 19.8 m, respectively, are given for each experiment in Tables 2 and 3. [In the case of experiments 7 and

TABLE 1. Summary of the experiments.

Experiment	r_M (km)	U (m s^{-1})	f (s^{-1} × 10^5)	$k = \frac{U}{Lf}$
1	30	5	7.5	0.92
2	30	6.7	10	0.92
3	60	10	7.5	0.92
4	30	10	7.5	1.85
5	30	13.3	10	1.85
6	30	6.7	5	1.85
7	60	5	7.5	0.46
8	60	7.5	7.5	0.69
9	30	5	7.5	0.92
10	30	7.5	7.5	1.38
11	30	10	7.5	1.85
12	30	12.5	7.5	2.31

TABLE 2. The maximum horizontal current found in the wake of the storm at a depth of 9.9 m; L and N denote linear and nonlinear experiment without mixing, respectively; M denotes nonlinear experiment with mixing. Note that only in experiments 7 and 8 are larger currents found in the region of forcing.

Experiment	Horizontal current (m s^{-1})			Maximum entrainment (m)	(nondimensional)			V_M (k)	$k = \frac{U}{Lf}$
	L	N	M		L	N	M		
1	3.5	2.4	1.5	47.7	2.8	2.8	2.8	3.0	0.92
2	2.8	1.9	1.4	35.7	3.0	2.9	3.0	3.0	0.92
3	3.8	2.6	1.8	38.3	3.0	3.0	3.0	3.0	0.92
4	2.4	1.7	1.5	23.7	3.8	3.9	4.0	4.0	1.85
5	1.9	1.3	1.2	19.3	4.0	4.0	4.0	4.0	1.85
6	3.5	2.6	1.9	34.5	3.7	4.0	4.0	4.0	1.85
7	1.9	1.6	0.8	59.2	0.8	0.9	0.9	0.9	0.46
8	3.1	2.1	1.3	46.5	1.9	1.8	1.8	1.8	0.69
9	3.5	2.4	1.5	47.7	2.8	2.8	2.8	3.0	0.92
10	3.2	2.3	1.8	32.1	3.8	4.0	4.2	4.0	1.38
11	2.4	1.7	1.5	23.7	3.8	3.9	4.0	4.0	1.85
12	1.9	1.4	1.3	20.1	3.8	4.0	4.1	3.9	2.31

8 (for which $k < 1$), higher values are achieved in the region of forcing.] Following (2.2a) and (2.2b), the horizontal current has been nondimensionalized by $(\tau_{max}L/\rho_0 H_M U)F_v$ [−9.9 m] and the vertical velocity by $(\tau_{max}/\rho_0 U)G_v$ [−19.8 m] for both the linear and nonlinear experiments without mixing. Note that F_v and G_v are given by (2.3a) and (2.3b), respectively. In the nonlinear experiments with mixing, the nondimensionalization follows (2.11) and (2.14); i.e., the horizontal current has been nondimensionalized by $(\tau_{max}L/\rho_0(H_M + \Delta h)U)$ and the vertical velocity by $(\tau_{max}/\rho_0 U)[z = 19.8 \text{ m}/(H_m + \Delta h)]$ where $(H_M + \Delta h)$ is the maximum value of h_E found by integrating (2.12) as part of the model solution. The corresponding maximum entrainment (Δh) is shown in each of Tables 2 and 3. Also given are the values of $V_M(k)$ and $W_M(k)$ given by (2.10) and calculated by numerically integrating the linear Ekman equations (2.1a) and (2.1b) with the wind stress τ given by (4.2) and using the same finite difference scheme as in the full numerical model.

The overall closeness of the nondimensional values in each case to the corresponding values of $V_M(k)$ and $W_M(k)$ demonstrates one of the purposes of this paper, i.e., it shows that the maximum horizontal current and vertical velocity in the wake of the storm can be calculated using the formulae (2.11) and (2.14), respectively; i.e., using a linear Ekman model to calculate $V_M(k)$ and $W_M(k)$ and a knowledge of that part of the change in the mixed layer depth due to entrainment, in this case Δh. It also demonstrates that at least in the cases considered, horizontal advection is not important as far as determining the magnitude of the response is concerned.

The nondimensional horizontal current and vertical velocity for the linear and nonlinear experiments with-

TABLE 3. As in Table 2, but for the maximum vertical velocity found in the wake of the storm at a depth of 19.8 m. Only in experiments 7 and 8 are larger vertical velocities found in the region of forcing.

Experiment	m s^{-1} × 10^3			Maximum entrainment (m)	Nondimensional			W_M (k)	$k = \frac{U}{Lf}$
	L	N	M		L	N	M		
1	1.55	1.07	0.70	47.7	4.5	4.5	4.8	4.9	0.92
2	1.21	0.79	0.61	35.7	4.7	4.4	4.8	4.9	0.92
3	0.83	0.56	0.42	38.3	4.8	4.7	5.2	4.9	0.92
4	0.85	0.55	0.46	23.7	4.9	4.6	4.5	5.0	1.85
5	0.66	0.43	0.40	19.3	5.1	4.8	4.8	5.0	1.85
6	1.21	0.77	0.58	34.5	4.7	4.3	4.5	5.0	1.85
7	0.61	0.51	0.27	59.2	1.8	2.1	2.1	2.0	0.46
8	0.71	0.53	0.32	46.5	3.1	3.3	3.3	3.2	0.69
9	1.55	1.07	0.70	47.7	4.5	4.5	4.8	4.9	0.92
10	1.09	0.74	0.58	32.1	4.8	4.6	4.9	5.2	1.38
11	0.85	0.55	0.46	23.7	4.9	4.6	4.5	5.0	1.85
12	0.67	0.42	0.38	20.1	4.9	4.4	4.4	5.2	2.31

out mixing are plotted on Fig. 1 to afford comparison with the analytic curves that were obtained using the greatly simplified wind stress field (2.17). It is clear that the numerical results, which are computed using the more realistic wind stress field (4.2), follow the basic shape of the analytic curves in both linear and nonlinear cases. Note that $\lim_{k\to\infty} V_M(k)$ has been fixed to be the same for both the numerical experiments and the analytic curve by our choice of L. On the other hand, $\lim_{k\to\infty} W_M(k)$ does not depend on the choice of L and can be calculated—it is given by (2.21). The numerically calculated value for the wind stress field (4.2) is 5.1.

2) THE HORIZONTAL STRUCTURE OF THE SOLUTIONS

Figure 3 shows the vertical velocity field at 19.8 m depth for each of experiments 1–6 in both linear and nonlinear experiments without mixing. The contours are drawn at intervals of $\frac{1}{6}$ the maximum response and the horizontal coordinates are stretched so that the area occupied by the storm appears the same in each case. It is clear that, when plotted in this way, i.e., in coordinates scaled with respect to the size of the storm, the horizontal structure of the response is essentially the same in each group of experiments with the same value of $k = U/Lf$—these are experiments 1, 2 and 3 for which $k = 0.92$ and experiments 4, 5 and 6 for which $k = 1.85$. This was one of the conclusions drawn in Section 2 about the response in the large, fast storm limit. Furthermore, the along-track wavelength of the oscillations left behind by the storm is close to the local inertial wavelength $2\pi U/f$ in each case, as can be seen by extending the integration sufficiently behind the storm, again indicating that the solutions are well approximated on this time scale by the large, fast limit.

The nonlinear distortions, which can be seen by comparing the plots for equivalent linear and nonlinear experiments, were described in Greatbatch (1984). Values for the parameters A_T and P_T, which measure the importance of the horizontal advection terms in the equations of motion, are given in Table 4 with the scale V in (2.15) taken to be the maximum horizontal current found in the wake of the storm in each case. Values calculated using (2.16) are also given, showing that these formulas provide a good means of measuring the importance of nonlinear effects in the wake.

3) THE VERTICAL STRUCTURE OF THE SOLUTIONS

So far, only the structure and amplitude of the solutions near the surface have been considered. Fig. 4a shows the vertical velocity field on a section across the storm track under the eye of the storm in the nonlinear version of experiment 1 (without mixing). This is at the beginning of the initial upwelling in response to the storm, as can be seen from Fig. 3a. It is clear that the vertical structure of the solution at this time is well described by that found in Section 2, i.e., by the function $Gv(z)$ defined in (2.3b). In particular, the upwelling is taking place throughout the depth of the ocean so that a description in terms of vertically propagating waves is clearly inappropriate (cf. Price, 1983). It is shown in Appendix B that the forced response to any fast or large disturbance [in the sense of (1.7)] does not feel the stratification and will extend throughout the depth of the ocean.

Figure 4b shows the vertical velocity structure during the second upwelling phase, again in the nonlinear version of experiment 1 (without mixing). It is clear that departures from the simple picture described in Section 2 are taking place, the maximum near 500 m depth being associated with the first baroclinic mode which is separating out from the solution. These departures are in association with the horizontal pressure gradient terms which were neglected in Section 2.

The vertical structure of the horizontal velocity field, on the same section as Fig. 4b, is shown in Fig. 4c. Although there is some departure from the simple picture given in Section 2, the response is basically surface trapped and given by the function $Fv(z)$ [cf. (2.3a)] at this time. Price (1983, 1984) give a detailed discussion of how horizontal currents are subsequently generated in the thermocline.

Figure 5 shows the temperature structure on a section across the storm track, again in the nonlinear version of experiment 1 (without mixing). Note once again, the large vertical structure of the upwelling response, extending throughout the thermocline. The bias to the right of the track, particularly evident in Fig. 5b, is a nonlinear effect.

5. Interpreting the results of observations and other numerical experiments

As an example, we consider the data set recorded by the EB-10 buoy during the passage of Hurricane Eloise of 1975 [Johnson and Withee (1978)]. This has been simulated by Price (1981) and here we use the model winds used by Price rather than the raw data recorded by the buoy (see Fig. 12 in Price's paper). We can then calculate the surface wind stress τ using the drag coefficient

$$c_D = (0.73 + 0.069V) \times 10^{-3} \tag{5.1}$$

and the bulk aerodynamic formula $\tau = \rho c_D V^2$, exactly as done by Price, where V is the wind speed (at 10 m height) in m s^{-1} and ρ is the density of air; (5.1) is essentially the composite form given by Garratt (1977).

Given this wind stress distribution, it is a simple matter to integrate (2.1a) and (2.1b); i.e.,

$$\left.\begin{aligned} Uu_\xi - fv &= X \\ Uv_\xi + fu &= Y \end{aligned}\right\}, \tag{5.2}$$

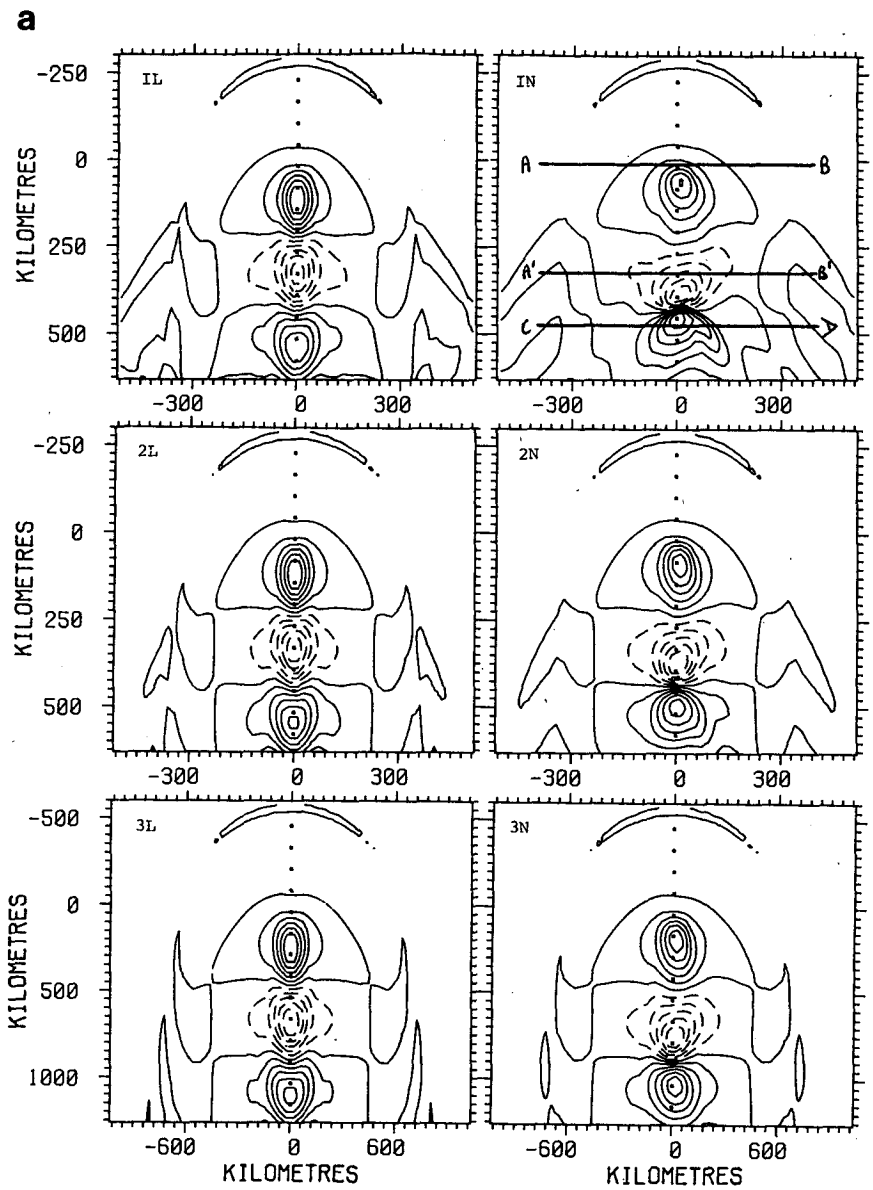

FIG. 3. The vertical velocity field at 19.8 m depth in each of (a) experiments 1, 2 and 3; and (b) experiments 4, 5 and 6: L indicates linear experiment (without mixing) and N nonlinear experiment (without mixing). The contour interval is $\frac{1}{6}$ of the maximum response in each case, the solid contours denoting upwelling and the dashed downwelling. The coordinates are measured in kilometers from the storm center, the along-track coordinate increasing behind the storm. The storm moves up the center of each figure, the storm track being shown by the dotted line. The zero contour is drawn as a solid line.

where $(X, Y) = (\tau_x, \tau_y)/\rho_0 H_I$ with $u = v = 0$ ahead of the storm. The translation speed U is 8.5 m s^{-1} in this case. Here H_I is fixed and can be assigned any value. If V_I is the maximum calculated horizontal current and D_I the maximum calculated horizontal divergence, then we know from (2.10) and (2.2a,b) that

$$V_I = \left(\frac{\tau_{\max} L}{\rho_0 H_I U}\right) V_M(k) \tag{5.3}$$

and

$$D_I H_I = \left(\frac{\tau_{\max}}{\rho_0 U}\right) W_M(k). \tag{5.4}$$

a. *Calculating the entrainment* Δh

Unfortunately, the mixed layer current was not measured by the EB-10 buoy. However, Price obtained a maximum in this current of $V_{\max} \approx 1.15$ m s^{-1}. We

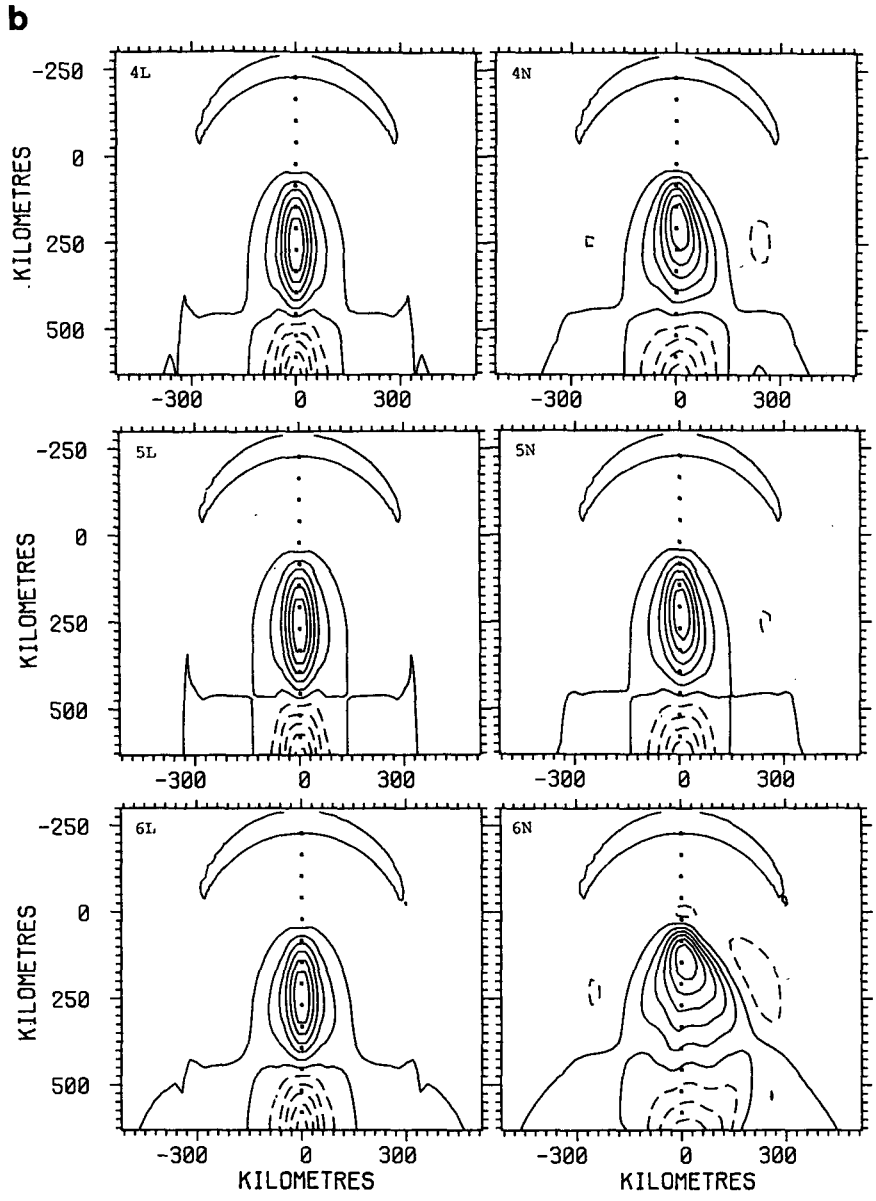

FIG. 3. (*Continued*)

saw in the last section that (2.11) can be used to calculate the maximum current in the wake—in this case $V_{\max}$. We can therefore write

$$V_{\max} = \left(\frac{\tau_{\max} L}{\rho_0 H_E U}\right) V_M(k), \tag{5.5}$$

where $H_E = H_M + \Delta h$, H_M being the initial mixed layer depth (taken to be 30 m in Price's experiments) and Δh the maximum entrainment due to the storm. [It is also assumed that h (mixed layer depth) $\ll H$ (ocean depth); this was used to establish (2.11)].

Combining (5.3) and (5.5), we deduce that

$$H_E = \frac{V_I H_I}{V_{\max}} \tag{5.6}$$

from which we can estimate the entrainment Δh. [Alternatively, if we know H_E then $V_{\max}$ can be calculated from (5.6)].

Substitution of appropriate values into (5.6), gives an estimate for H_E of 98 m and of $\Delta h = H_E - H_M$ of 68 m. This seems to agree quite well with what Price actually found (see Fig. 19 in Price's paper). This shows plots of mixed layer depth h and η_1 the upwelling just below the base of the mixed layer. Here, H_E, the max-

TABLE 4. The importance of the nonlinear terms as measured by the parameters A_T and P_T and as estimated by (2.16) in the nonlinear experiments without mixing.

Experiment number	$A_T = \frac{V}{U}$	$\left(\frac{\tau_{max}L}{\rho_0 H_M U^2}\right)V_M$ (k)	$P_T = \frac{V}{Lf}$	$\left(\frac{\tau_{max}}{\rho_0 H_M U f}\right)V_M$ (k)	$k = \frac{U}{Lf}$
1	0.5	0.5	0.4	0.5	0.92
2	0.3	0.3	0.3	0.3	0.92
3	0.3	0.3	0.2	0.2	0.92
4	0.2	0.2	0.3	0.3	1.85
5	0.1	0.1	0.2	0.2	1.85
6	0.4	0.4	0.7	0.7	1.85
7	0.3	0.3	0.1	0.1	0.46
8	0.3	0.3	0.2	0.2	0.69
9	0.5	0.5	0.4	0.5	0.92
10	0.3	0.3	0.4	0.4	1.38
11	0.2	0.2	0.3	0.3	1.85
12	0.1	0.1	0.3	0.3	2.31

imum of $(h + \eta_1)$, seems to be a little over 90 m, as can be seen by superposing the two plots.

b. *Calculating the sea surface temperature response*

Given the entrainment, we can estimate the sea surface temperature response and compare it with what Price actually found in his model. The equation for the heat content of the wind-mixed layer is

$$\left(\frac{dQ}{dt}\right)_{mix} = \frac{hDT_s}{Dt} + \left(\frac{dh}{dt}\right)_{mix}(T_s - T_{-h}), \quad (5.7)$$

where D/Dt is the total derivative following a fluid particle, $-(dQ/dt)_{mix}$ the sensible and latent heat flux to the atmosphere, T_s the sea surface temperature (i.e., the temperature of the wind-mixed layer) and $T_s - T_{-h}$ is the temperature difference across the base of the wind-mixed layer. It is convenient to define h_E and h_D as in (2.6) so that

$$\left.\begin{aligned} \frac{Dh_E}{Dt} &= \left(\frac{dh}{dt}\right)_{mix} \\ h_E|_{\text{ahead of storm}} &= H_M \\ h_D &= h_E - h \end{aligned}\right\}, \quad (5.8)$$

where H_M is the depth of the wind-mixed layer ahead of the storm.

In Price's model, the temperature T_{-h} below the wind-mixed layer varies linearly with depth and with gradient $\beta = -0.125°C\ m^{-1}$. We can see from (2.3b) that provided h_E is always small compared with the total depth H of the ocean, then the upwelling below the wind-mixed layer can be assumed to be independent of depth so that we have

$$T_{-h} = T_0 + \beta h_E. \quad (5.9)$$

In Price's model, $T_0 = 32.45°C$. Note that if there were no upwelling, then $h_D = 0$ in which case $h = h_E$ in (5.9).

Equation (2.11) uses the assumption that $h_D \ll h_E$. We can apply the same idea to (5.7)[6] in which case we have

$$\left(\frac{dQ}{dt}\right)_{mix} = h_E\frac{DT_s}{dt} + \left(\frac{dh}{dt}\right)_{mix}(T_s - T_{-h}).$$

Using (5.8) and (5.9), this equation can be written as

$$\left(\frac{dQ}{dt}\right)_{mix} = \frac{Da}{Dt} - \beta h_E\frac{Dh_E}{Dt}, \quad (5.10)$$

where $a = h_E(T_s - T_{-h})$. (5.10) can be integrated following a fluid particle under the storm to give

$$\int\left(\frac{dQ}{dt}\right)_{mix}dt = (a - a_0) + \frac{1}{2}\beta(H_M^2 - h_E^2), \quad (5.11)$$

where a_0 is the value of $a = h_E(T_s - T_{-h})$ ahead of the storm.

Knowing a_0, β, H_M, the entrainment $\Delta h = h_E - H_M$ and the sensible and latent heat transfer to the atmosphere, (5.11) gives $a = h_E(T_s - T_{-h})$ behind the storm and hence the sea surface temperature T_s. Substituting values from Price's model and the entrainment depth $h_E = 98$ m previously estimated, we obtain $T_s = 25.6°C$. This corresponds to a maximum surface cooling of 3.2°C which is close to that found by Price (see his Fig. 15b).

Note that of the information needed to obtain this estimate from (5.11), a_0, β and H_M refer to the ocean ahead of the storm with only $\int (dQ/dt)_{mix}dt$ and the

[6] It turns out that, in general, this is not as good an approximation as it is for the horizontal and vertical velocity fields. The reader is referred to Greatbatch (1984) for a detailed discussion of the sea surface temperature response.

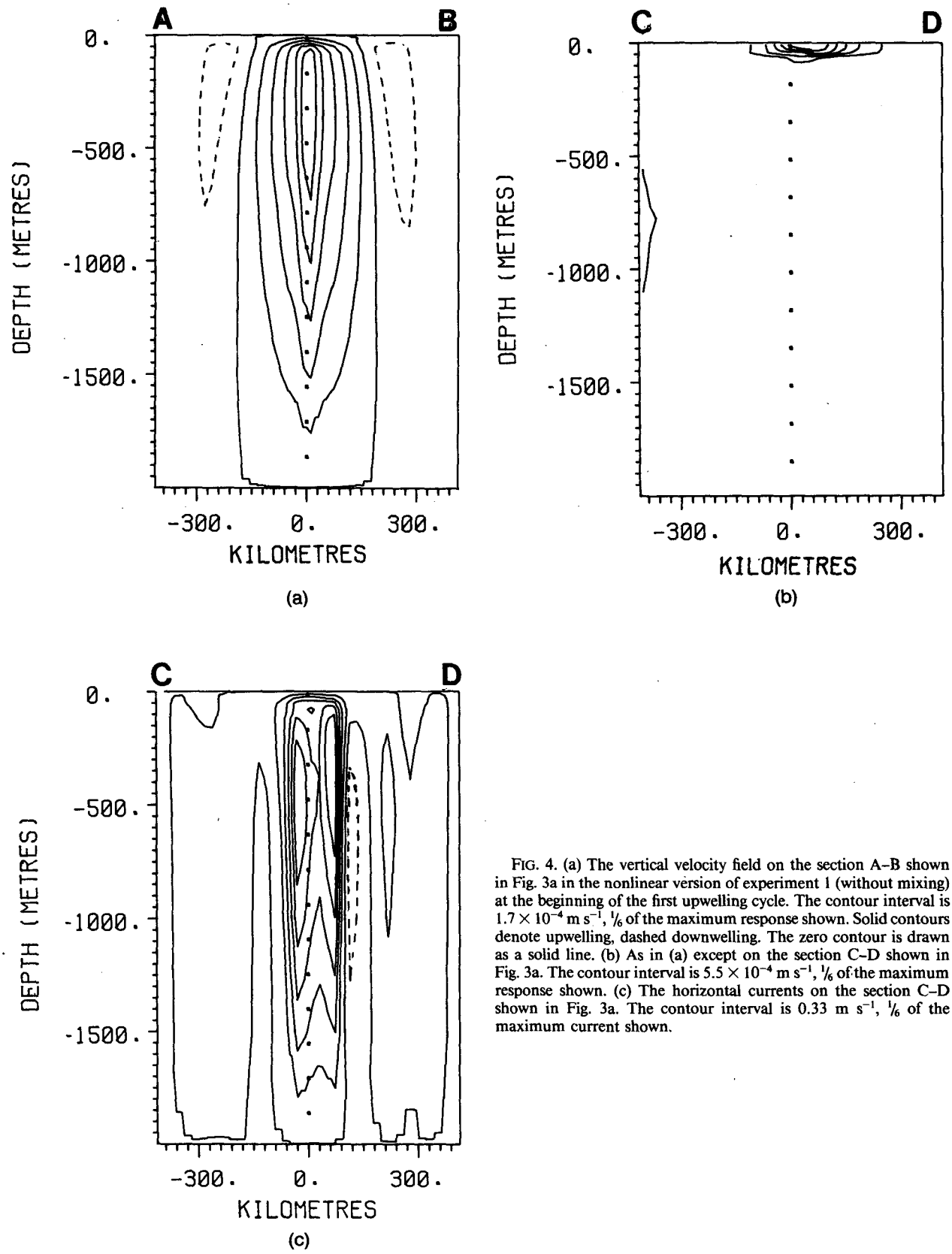

FIG. 4. (a) The vertical velocity field on the section A–B shown in Fig. 3a in the nonlinear version of experiment 1 (without mixing) at the beginning of the first upwelling cycle. The contour interval is 1.7×10^{-4} m s^{-1}, 1/6 of the maximum response shown. Solid contours denote upwelling, dashed downwelling. The zero contour is drawn as a solid line. (b) As in (a) except on the section C–D shown in Fig. 3a. The contour interval is 5.5×10^{-4} m s^{-1}, 1/6 of the maximum response shown. (c) The horizontal currents on the section C–D shown in Fig. 3a. The contour interval is 0.33 m s^{-1}, 1/6 of the maximum current shown.

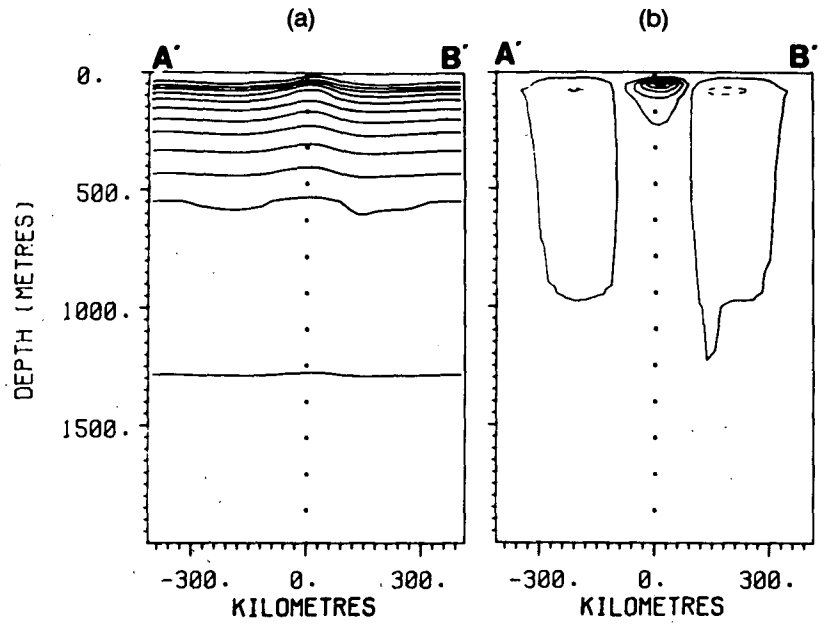

FIG. 5. (a) The temperature field on the section A'B' shown in Fig. 3a, isotherms at intervals of 2°C. (b) As in (a) except that here the change in temperature from the initial state is shown. Warming is indicated by dashed contours; cooling by solid contours. The contour interval is 1°C. The zero contour is shown as a solid line.

entrainment depth h_E referring to the action of the storm. Of these two, the former is a small term in (5.11). The sensible and latent heat transfer found by Price in his model was used in the calculation above. If, however, we put this [i.e., $\int (dQ/dt)_{\text{mix}} dt$] equal to zero, we obtain $T_s = 25.9$°C.

We could do this calculation in reverse. Knowing the sea surface temperature response, we can calculate the entrainment depth h_E from (5.11). Then, knowing the surface wind stress field and hence V_I in (5.6), we calculate the maximum current in the mixed layer, $V_{\max}$.

c. *Calculating the upwelling*

It was also shown in the last section that the maximum vertical velocity in the wake $W_{\max}$ is given by (2.14). If we assume that (2.14) holds here, then by using (5.4), we have

$$W_{\max} = \left(\frac{h}{H_E}\right) D_I H_I. \tag{5.12}$$

Superposing Fig. 19a and Fig. 18b from Price's paper, we see that the mixed layer depth h at the position where the vertical velocity w_1 at the base of the wind

TABLE 5. The maximum horizontal current and maximum entrainment found in the wake of the storm and along the storm track in each of the nonlinear experiments with mixing. The nondimensional current amplitude is compared with that found in equivalent linear and nonlinear Ekman models.

Experiment number	Maximum current (m s^{-1})	Maximum entrainment m	Nondimensional current	Nondimensional Ekman current	
				linear	nonlinear
1	1.4	45.0	2.6	2.5	2.5
2	1.2	34.3	2.5	2.5	—
3	1.5	36.5	2.5	2.5	—
4	0.93	22.2	2.4	2.6	2.2
5	0.76	18.3	2.5	2.6	—
6	1.2	31.0	2.4	2.6	—
7	0.60	56.8	0.6	0.8	0.7
8	1.1	44.6	1.5	1.5	1.4
9	1.4	45.0	2.6	2.5	2.5
10	1.5	30.5	3.4	2.9	3.4
11	0.93	22.2	2.4	2.6	2.2
12	0.72	18.8	2.2	2.3	2.0

mixed layer is a maximum is 70 m. Taking the estimated value for H_E from (i) of 98 m, it follows that the maximum value of W_1 given by (5.7) is $(70/98)D_IH_I$ (it is also assumed that $h \ll H$ once again). The calculated value for D_IH_I is 1.76×10^{-3} m s^{-1}, so that $(70/98)D_IH_I$ is 1.3×10^{-3} m s^{-1} which is the value given by Price in Fig. 18b of his paper. (Superposing Fig. 19b and Fig. 18b suggests that $\eta_1 \approx 15$ m where W_1 has its maximum value of 1.3×10^{-3} m s^{-1}. This implies a local value of h_E of 85 m. $(70/85)D_IH_I$ is 1.4×10^{-3} m s^{-1}).

d. *Observations at a fixed point*

Tables 2 and 3 both referred to the maximum horizontal and vertical velocities, respectively. The effect of the nonlinear terms, however, is to displace the positions of these maxima between equivalent linear and nonlinear cases. It is of interest, therefore, to examine the importance of this effect, given that observations measured by a buoy usually refer to a fixed point and it may not be appropriate to use the linear Ekman equations (5.2) to draw conclusions about the amplitude of the response at that point.

Table 5 shows the maximum current found in the wake of the storm and along the storm track in each of the twelve experiments with mixing described in Section 4. These values nondimensionalized by $[\tau_{max}L/\rho_0(H_M + \Delta h)U]$ [cf. (2.11)] are also given where Δh is the maximum entrainment found along the storm track (also given in Table 5). Also given are the equivalent nondimensional values obtained by integrating the linear Ekman equations (5.2) and the nonlinear Ekman equations

$$\left.\begin{aligned} \frac{Du}{Dt} - fv &= \left(\frac{\tau_x}{\rho_0 H_I}\right) \\ \frac{Dv}{Dt} + fu &= \left(\frac{\tau_y}{\rho_0 H_I}\right) \end{aligned}\right\}. \tag{5.13}$$

Obviously, the importance of the nonlinear effect depends now on our choice of H_I. In the cases presented, it has been fixed at 50 m.

A particularly interesting case study is that of experiment 10 in which there is clearly a large discrepancy in the current amplitude along the storm track that is predicted by the linear Ekman equations, a discrepancy which is removed when we consider the nonlinear Ekman equations. Fig. 6 shows the horizontal currents at the surface in each of linear, nonlinear (without mixing) and nonlinear with mixing versions of experiment 10. Note how in the nonlinear case, the band in which the maximum current amplitude is found first bends away from the storm track, but then bends back again and almost reaches the track at the end of the integration, significantly contributing to the maximum given in Table 5. In the linear case, the band of maximum current remains at a fixed displacement

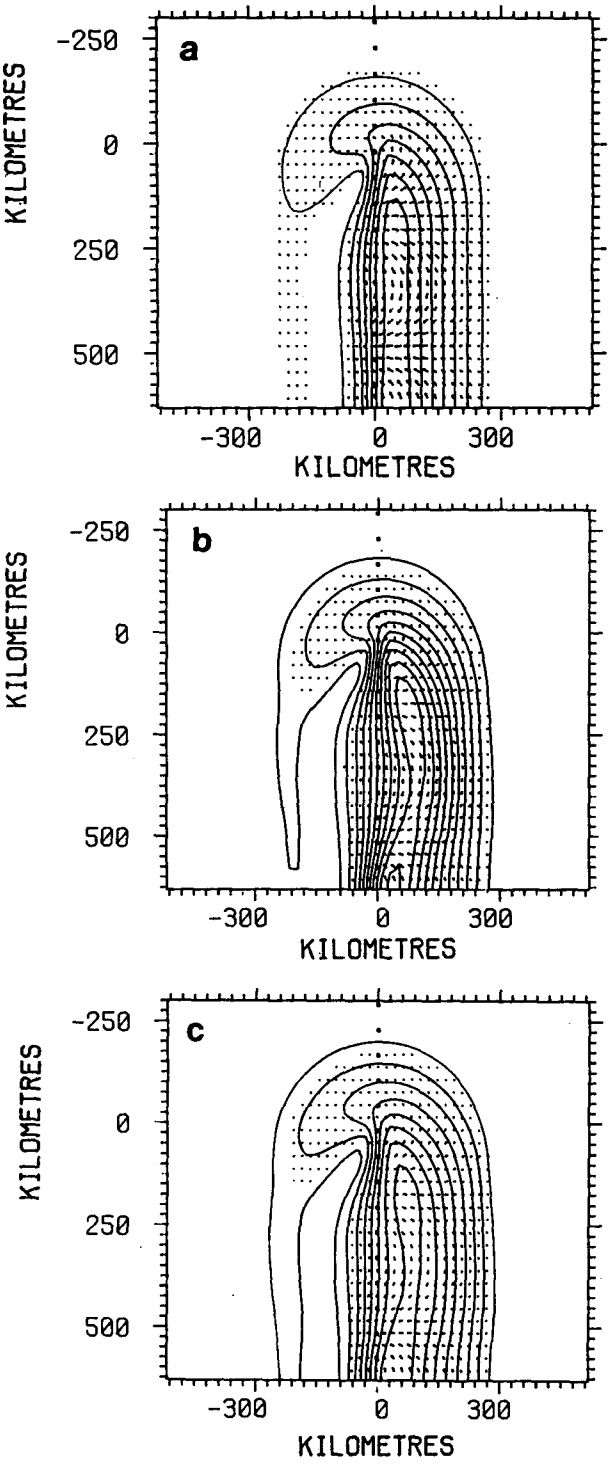

FIG. 6. (a) The horizontal current field in the linear version of experiment 10 (without mixing). The contours are drawn at intervals of 40 cm s^{-1} and the arrows denote the vector velocity. The coordinates are measured in kilometers from the center of the storm, the along-track coordinate increasing behind the storm. The storm moves up the center of the figure. (b) As in (a) except for the nonlinear version of experiment 10 (without mixing). The contours are at intervals of 20 cm s^{-1}. (c) As in (a) except for the nonlinear version of experiment 10 with mixing. The contour interval is 20 cm s^{-1}.

away from the storm track. [These features of the nonlinear solution have been explained by Greatbatch (1983) who showed that to a first approximation the fluid particles move in inertial circles in the wake of the storm. The maximum current of 1.8 m s^{-1} given in Table 2 for the mixing version of experiment 10 corresponds to an inertial circle of radius 24 km. It is clear from Fig. 6 that the current amplitude near the storm track varies significantly over this distance, again demonstrating the need to consider the nonlinear equations (5.13).]

In conclusion, when interpreting results or observations at a fixed point, we note that it can be important to consider nonlinear effects and to consider the nonlinear Ekman equations (5.13) rather than the linear Ekman equations (5.2).

6. Summary and conclusions

The two purposes of this paper set out in the Introduction have been achieved: first, to present a new and efficient multilevel numerical model for calculating the response to a moving storm (Section 3) and second, to show how, on a time scale of a few inertial periods following the onset of the storm, the maximum horizontal and vertical velocities found in the wake can be calculated using a linear Ekman model and a knowledge of that part of the change in the depth of the mixed layer due to entrainment. This second result is expressed by Eqs. (2.11) and (2.14) and was verified using the results generated by the multilevel numerical model over a range of experiments described in Section 4 and applied to an interpretation of Price's (1981) model results in Section 5. It was also demonstrated in Section 5 that when considering model results or observations at a fixed point, it is important to consider the effect of horizontal advection.

An important feature of the numerically generated solutions described in Section 4 is the confinement of the horizontal currents near the surface although the large vertical scale of the vertical velocity field extends throughout the depth of the ocean. These were features found in Section 2 when considering the structure of the response in the limit of large, fast storms. In this case, the vertical velocity, which is just the inertial pumping, varies linearly from the base of the wind-mixed layer to the ocean floor. This is discussed further in Appendix B where it is shown that the wind forcing need only be large or fast, in the sense of (1.7), for the response to extend throughout the depth of the ocean in this way. We have also seen that on the time scale considered—a few inertial periods following the arrival of the storm—the horizontal structure of the response, in coordinates scaled with respect to scale L of the storm, is given by the value of the parameter $k = U/Lf$. Here U is the translation speed of the storm and f the Coriolis parameter. The nondimensional functions $V_M(k)$ and $W_M(k)$ which we used in (2.11) and (2.14) to calculate the magnitude of the response, also depend only on k.

We have seen that (2.11) and (2.14) can be used to calculate the maximum horizontal and vertical velocities in the wake of the storm. These involve knowledge of that part of the change in mixed layer depth due to entrainment. A discussion of how this can be calculated is given in Greatbatch (1984). It should be noted, however, that although the fundamental equation (2.9), on which (2.11) and (2.14) are based, involved taking the limit $h_D/h_E \to 0$ [see (2.6) for the definitions of h_E and h_D], this does not mean that we are neglecting the effect of upwelling on h_E [alternatively on the rate of entrainment of water into the wind-mixed layer $(dh/dt)_{\text{mix}}$]. In fact, as shown in Greatbatch (1984) (see Table 4 in that paper), h_E can be significantly increased by the effect of storm induced advection; in particular, upwelling.

Acknowledgments. I should like to thank Dr. A. E. Gill for his constant encouragement and advice, and also Dr. S. J. Hogan who provided some useful comments on an early version of this manuscript. I am also grateful to Dr. S. G. H. Philander and Dr. I. Orlanski of the Geophysical Fluid Dynamics Laboratory, Princeton, for stimulating discussions that led to the writing of Appendix B.

APPENDIX A

An Alternative Formulation of the Limit of Large, Fast Storms

Two alternative nondimensionalizations of the equations are given depending on whether cross-track or along-track derivatives are more important, i.e., $k > 1$ or $k < 1$, respectively. The scales chosen are those appropriate to the large, fast storm limit found in Section 2. In particular, nondimensional variables, denoted by a prime, are defined by

$$\xi = \frac{U\xi'}{f}; \quad y = Ly'; \quad z = H_M z';$$

$$(u, v) = V(u', v'); \quad w = Ww'; \quad \theta = \left(\frac{WN_0^2}{g\alpha f}\right)\theta'$$

$$p = \left(\frac{WN_0^2 H_T}{f}\right)p'.$$

When

$$\left.\begin{aligned} k > 1, \quad W &= \frac{VH_M}{L} \\ k < 1, \quad W &= \frac{VH_M f}{U} \end{aligned}\right\}.$$

The linearized momentum equations, written in terms of these variables, are (dropping primes)

TABLE 6. Values of E_1 and E_2, which measure the importance of the horizontal pressure gradient terms in the momentum equations, calculated for each experiment (without mixing). $N_0 = 1.5 \times 10^{-2}$ s^{-1}, $H_T = 550$ m and $L = 2.4\ r_M$ [cf. (4.3)]. Note that E_2 is the important parameter when $k < 1$, E_1 when $k > 1$ and E_1 and E_2 are related by $E_1 = k^2 E_2$.

Experiment number	$E_1 = N_0^2 H_M H_T / L^2 f^2$		$E_2 = N_0^2 H_M H_T / U^2$	
	Linear	Nonlinear	Linear	Nonlinear
1	0.15	0.21	0.18	0.26
2	0.08	0.12	0.10	0.15
3	0.04	0.05	0.05	0.07
4	0.15	0.21	0.05	0.07
5	0.08	0.12	0.03	0.04
6	0.33	0.47	0.10	0.15
7	0.04	0.05	0.18	0.26
8	0.04	0.05	0.08	0.12
9	0.15	0.21	0.18	0.26
10	0.15	0.21	0.08	0.12
11	0.15	0.21	0.05	0.07
12	0.15	0.21	0.03	0.04

1) $k > 1$

$$\left.\begin{aligned} u_\xi - v &= \frac{1}{k} E_1 p_\xi + X \\ v_\xi + u &= -E_1 p_y + Y \end{aligned}\right\},$$

2) $k < 1$

$$\left.\begin{aligned} u_\xi - v &= E_2 p_\xi + X \\ v_\xi + u &= -k E_2 p_y + Y \end{aligned}\right\},$$

where $E_1 = N_0^2 H_M H_T / (L^2 f^2)$ and $E_2 = N_0^2 H_M H_T / U^2$. The limit of large storms then corresponds to the limit in which $E_1 = 0$ and the limit of fast storms to the limit in which $E_2 = 0$. Clearly E_1 and E_2 correspond to the ratios given in (1.7) with $c = (N_0^2 H_M H_T)^{1/2}$ being a representative baroclinic wave speed, effectively amalgamating the discrete set of wave speeds $c_1, c_2 \cdots, c_n, \cdots$ used previously.

Values of E_1 and E_2 appropriate to each of the 12 experiments described in Section 4 are given in Table 6. Representative values chosen for N_0 and H_T are 1.5×10^{-2} s^{-1} and 550 m, respectively. [A problem in choosing N_0 is the wide variation over the depth of the ocean in the buoyancy frequency N. It is important to choose N_0 so that $c = 0$ (1 m s^{-1}).] H_M is 35 m in the linear and 50 m in the equivalent nonlinear experiments.

APPENDIX B

A Note Concerning the Depth of Penetration of the Ocean Response to Wind Forcing

A feature of the solutions found in the limit of large, fast storms discussed in Section 2 and of the numerical results presented in Section 4 (see Fig. 4a, for example) is that the response extends throughout the depth of the ocean and does not seem to propagate down from the surface in the form of waves. In this section, we show that *this deep response is forced and depends only on the storm being either fast in the sense of (1.7b) or large in the sense of (1.7a).* Consequently, *in either limit a description in terms of vertically propagating waves is inappropriate.* It follows that, because these limits are defined in terms of the baroclinic wave speeds c_n [or, equivalently the wave speed $c = (N_0^2 H_M H_T)^{1/2}$ introduced in Appendix A], *it is precisely these wave speeds which measure the penetrability of the ocean* and not the stratification immediately below the surface mixed layer, as suggested by the vertically propagating wave approach. To see how this can be misleading, we note that the maximum buoyancy frequency associated with the temperature profile (4.1) is 1.9×10^{-2} s^{-1}. If the buoyancy frequency had this uniform value throughout the depth of the ocean (2000 m in this case), then the wave speed associated with the first baroclinic mode would be 12 m s^{-1} and the entire response to a storm translating at 5 m s^{-1} would be completely different from that presented in this paper. It follows that consideration of only the upper, highly stratified part of the ocean, can be misleading.

We begin by showing that only fast storms are sufficient to produce a deep response. Fig. 7 is the equivalent of Fig. 4a but for a storm of one-tenth the size—r_M in (4.2) is 3 km, as against the previous 30 km. It is clear that the initial response extends throughout the depth of the ocean, as it did before. To see why this feature does not depend on storm size, consider the equations for a single baroclinic mode, as given according to linear theory

$$(U^2 - c^2)\eta_{\xi\xi} - c^2 \eta_{yy} + f^2 \eta = \mathcal{F}, \qquad \text{(B1)}$$

where η corresponds to the interface displacement in a two-layer model and $\mathcal{F}$ represents the forcing. The solution consists of a particular integral—the forced response, depending on $\mathcal{F}$—and a free wave solution that satisfies (B1) with $\mathcal{F} \equiv 0$.

We concentrate on the particular solution with the same horizontal scale L as the forcing $\mathcal{F}$. The terms $c^2\eta_{\xi\xi}$ and $c^2\eta_{yy}$ are then of the same order of magnitude in (B1) and both will be small compared with $U^2\eta_{\xi\xi}$ if $U^2 \gg c^2$. In the fast storm limit ($U^2 \gg c^2$), this solution satisfies

$$U^2 \eta_{\xi\xi} + f^2 \eta = \mathcal{F}. \qquad \text{(B2)}$$

Summing over all baroclinic modes, it follows that η has the same vertical structure as $\mathcal{F}$—this is just $Gv(z)$ defined by (2.3b). This forced response, therefore, extends throughout the depth of the ocean and a *description in terms of vertically propagating waves is inappropriate.*

The same conclusion follows whenever the forcing has a larger scale in y (perpendicular to the direction

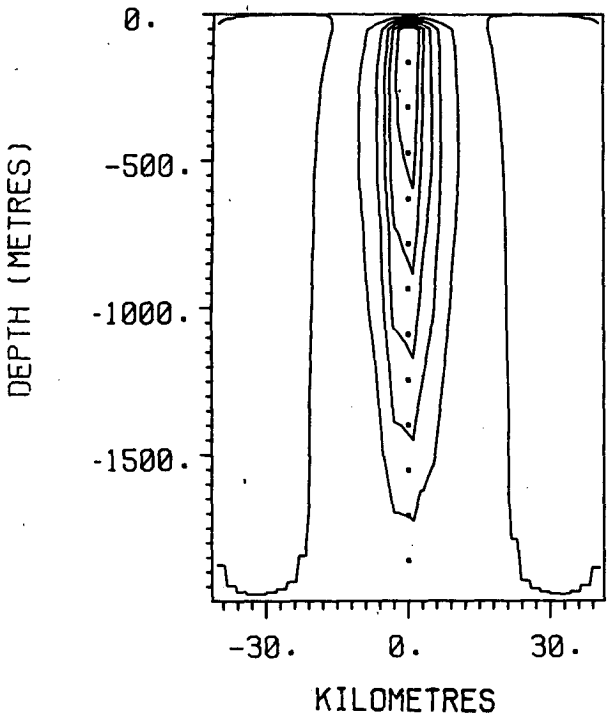

FIG. 7. The vertical velocity field immediately following the passage of the eye of a storm of one-tenth the horizontal scale that was used to produce Fig. 4a. This is the initial response in the vertical velocity field. The contour interval is 1.1×10^{-4} m s^{-1} which is $\frac{1}{6}$ of the maximum response shown. Solid contours here denote downwelling and dashed upwelling. The zero contour is drawn as a solid line.

of motion) than in ξ (the direction of motion)—this ensures that derivatives in ξ are more important than those in y in (B1). An example of such forcing is an atmospheric front.

Similarly for a large storm, the particular solution to (B1) with the same horizontal scale as the forcing $\mathcal{F}$ will again satisfy (B2) with this equation reducing to

$$f^2\eta = \mathcal{F}, \tag{B3}$$

when $U \leqslant O(c)$. The forced response therefore extends throughout the depth of the ocean as before. In particular, the response to a stationary storm that is "large" in the sense of (1.7a) will also extend throughout the depth of the ocean. [Note the large vertical scale of the vertical velocity field computed for a stationary storm by Adamec *et al.* (1981).]

REFERENCES

Adamec, D., R. L. Elsberry, R. W. Garwood Jr. and R. L. Haney, 1981: An embedded mixed layer–ocean circulation model. *Dyn. Atmos. Oceans,* **6,** 69–96.

Arakawa, A., and V. R. Lamb, 1977: Computational design of the UCLA General Circulation Model. *Methods in Computational Physics,* Vol. 17, J. Chang, Ed., Academic Press.

Chang, S. W., and R. A. Anthes, 1978: Numerical simulation of the ocean's non-linear, baroclinic response to translating hurricanes. *J. Phys. Oceanogr.,* **8,** 468–480.

Elsberry, R. L., T. S. Fraim and R. M. Trapnell, 1976: A mixed layer model of the oceanic thermal response to hurricanes. *J. Geophys. Res.,* **81,** 1153–1162.

Friese, L. V., 1977: Response of the upper ocean to Hurricane Eloise. M.S. thesis, U.S. Naval Postgraduate School, Monterey, CA.

Garratt, J. R., 1977: Review of drag coefficients over oceans and continents. *Mon. Wea. Rev.,* **105,** 915–929.

Geisler, J. E., 1970: Linear theory of the response of a two-layer ocean to a moving hurricane. *Geophys. Fluid Dyn.,* **1,** 249–272.

Gill, A. E., 1982: *Atmosphere-Ocean Dynamics. International Geophysics Series,* Vol. 30, Academic Press, 662 pp.

——, and A. J. Clarke, 1974: Wind-induced upwelling, coastal currents and sea-level changes. *Deep-Sea Res.,* **21,** 325–345.

——, and J. S. Turner, 1976: A comparison of seasonal thermocline models with observation. *Deep-Sea Res.,* **23,** 391–401.

Greatbatch, R. J., 1980: The response of the ocean to a moving hurricane. Ph.D. dissertation, University of Cambridge, 327 pp.

——, 1983: On the response of the ocean to a moving storm: The nonlinear dynamics. *J. Phys. Oceanogr.,* **13,** 357–367.

——, 1984: On the response of the ocean to a moving storm: The sea-surface temperature response. Submitted to *J. Phys. Oceanogr.*

Johnson, A., and G. W. Withee, 1978: Ocean data buoy measurements of Hurricane Eloise. *J. Mar. Technol. Soc.,* **12,** 14–20.

Martin, P. J., 1982: Mixed-layer simulation of buoy observations taken during hurricane Eloise. *J. Geophys. Res.,* **87,** 409–427.

O'Brien, J. J., 1967: The non-linear response of a two-layer baroclinic ocean to a stationary, axially symmetric hurricane: Part II. Upwelling and mixing induced by momentum transfer. *J. Atmos. Sci.,* **24,** 208–215.

——, 1969: The response of the ocean to a slowly moving hurricane. *Ann. Hydrogr. Mar. Meteor.,* **4,** 60–65.

—— and R. O. Reid, 1967: The non-linear response of a two-layer, baroclinic ocean to a stationary, axially symmetric hurricane. Part I: Upwelling induced by momentum transfer. *J. Atmos. Sci.,* **24,** 197–207.

Price, J. F., 1981: On the upper ocean response to a moving hurricane. *J. Phys. Oceanogr.,* **11,** 153–175.

——, 1983: Internal wave wake of a moving storm. Part I: Scales, energy budget and observations. *J. Phys. Oceanogr.,* **13,** 949–965.

——, 1984: Internal wave wake of a moving storm. Part II: Parameter dependence. Submitted to *J. Phys. Oceanogr.*

Schramm, W. G., 1979: Airborne expendable bathythermograph observations immediately before and after the passage of typhoon Phyllis in August of 1975. Dept. of Navy, NAVENVPREDRESFAC, Tech. Rep. 79-05, 42 pp.

Wells, N. C., 1979: A coupled ocean-atmosphere experiment: The ocean response. *Quart. J. Roy. Meteor. Soc.,* **105,** 355–370.